Complete Set of Critical Points on the $C_{60}H^+$ Potential Energy Surface

Martin Šala,[†,‡] Milan Hodošček,[§] Sundaram Arulmozhiraja,[||] and Toshihiro Fujii*[,†]

Department of Chemistry, Faculty of Sciences and Engineering, Meisei University, Hodokubo 2-1-1, Hino, Tokyo 1813-0033, Japan, National Institute of Chemistry, Hajdrihova 19, 1000 Ljubljana, Slovenia, and National Institute for Materials Science, 1-2-1 Sengen, Tsukuba, Ibaraki 305-0047, Japan

Received: November 18, 2008; Revised Manuscript Received: January 26, 2009

To calculate the proton affinity of fullerene (C_{60}), density functional theory was used to determine the global minimum energy structures of both fullerene and its protonated forms. Vibrational frequency calculations were used to check the nature of these predicted structures. In the protonation of C_{60} in the gas phase, the proton preferentially lies above the carbon atoms at a distance of 1.10 Å, which suggests a bond of covalent nature. The proton affinity for fullerene was calculated as 201.8 kcal/mol, compared with the experimental value between 204 and 207 kcal/mol obtained by proton-transfer bracketing studies using Fourier transform mass spectrometry. All five transition states for intramolecular proton transfer in fullerene were found, three for the first time. The activation energy (E_a) barriers for proton migration were calculated and ranged from 27 to 90 kcal/mol. Different functional groups attached to fullerenes, and their influence on E_a values are discussed, as are all the possible proton transfers for nonfunctionalized fullerenes.

Introduction

Proton conductivity is an essential feature of functional materials for polymer electrolyte fuel cells (PEFCs). Proton conductivity in C_{60}-based solid electrolyte was first investigated 20 years ago,[1] but recent studies are of proton conductivity in functionalized C_{60}. The Sony Corporation confirms that functionalized fullerenes can be used successfully as functional materials for PEFCs.[2] The latest research shows that PEFCs at elevated temperatures increase carbon monoxide tolerance and allow the production of smaller systems.[3] Hence, potential materials for PEFCs should have a high proton conductivity in the widest temperature range, possibly at low humidity, and be as robust and stable as possible. However, loss of water from membranes at higher temperatures makes conserving the proton conductivity at low humidity a crucial feature of functional materials for PEFCs. Hara et al.[4] report that Nafion-type membranes lose their proton conductivity with loss of water from the membranes, and this also occurs with other promising materials.[5] Other reports on promising materials with high proton conductivity do not give data for conductivity at low humidity, and therefore it is unclear whether these materials retain high proton conductivity at the high temperatures at which no water is present.[4] Despite much effort and the substantial progress achieved to improve the proton conductivity of membranes at low humidity,[6,7] further improvement is still needed. Recent advances in the use of functionalized C_{60} for PEFCs at low humidity show some promising results[8−12] and also address some issues raised by the work of Hinokuma and Ata[13] on polyhydroxyl hydrogen sulfated fullerene, $C_{60}(OH)_n(OSO_3H)_{12-n}$ ($n \approx 6$). Their investigation did not show whether the conductivity of their fullerene resulted from the functional groups of the fullerene or was because the fullerene itself possessed a conductive nature. When these fullerene derivatives were mixed in a polymer, the conductivity dropped significantly. Furthermore, decomposition of these fullerene derivatives at around 100 °C made it problematic to fabricate a practical composite membrane.

The lower the activation energy (E_a) barrier for proton transfer, the higher the proton conductivity. To determine the E_a, the transition state in the proton migration reaction has to be identified. The activation energies for proton, intermolecular, and intramolecular transfers are already determined theoretically for C_{60}, but not all of the transition states are.[14] Low values of E_a for fullerene, around 30 kcal/mol, denote that migration on and between fullerene molecules is facile, and hence it possesses high proton conductivity. Proton conductivity experimentally obtained for functionalized fullerenes can be as high as 10^{-2} S cm^{-1}.[2,13,14] A low E_a is connected to the distance between the two sites that take part in the proton-transfer reaction. It is important for a molecule to possess high proton conductivity, that this distance should be neither too short nor too long, and the ideal value lies somewhere above 2.6 Å, as Kreuer discusses in his review.[15] Fullerenes are suitable as PEFC material because of their potentially high proton conductivity.[8,13,16] Fullerenes can be functionalized, and therefore their properties can be fine-tuned by selecting appropriate functional groups for functionalization. Additionally, fullerenes are very suitable for use as a PEFC material because they are thermally extremely stable and their proton conductivity is less dependent on humidity than that of other materials currently used in PEFCs. The conclusion is that low humidity would not affect the proton conductivity of functionalized fullerenes, as found for some otherwise promising materials,[5] because all the calculations were made in a vacuum gas phase. However, the experimental data do not establish why functionalized fullerenes have good conductivity (see above). Thus, it is important to determine all possible transition states and their E_a values. For highly functionalized

* To whom correspondence should be addressed. Phone and fax: +81425915595. E-mail: fujii@chem.meisei-u.ac.jp.
† Meisei University.
‡ JSPS Fellow from the Faculty of Chemistry and Chemical Technology, University of Ljubljana, Ljubljana, Slovenia.
§ National Institute of Chemistry.
|| National Institute for Materials Science.

10.1021/jp8101145 CCC: $40.75 © 2009 American Chemical Society
Published on Web 03/03/2009

fullerenes, the proton-transfer reaction with the smallest E_a is not possible, and therefore other proton-transfer reactions come into effect.

To understand all the reactions that involve proton transfer, it is essential to know the proton affinity (PA), a fundamental property of molecules. PA is a measure of the gas-phase basicity of the anion or neutral molecule that accepts the proton. Strikingly, PA has been neither determined exactly nor calculated for fullerene. Experimental values reported from proton-transfer bracketing studies in Fourier transform mass spectrometry are between 204 and 207 kcal/mol.[17] Nevertheless, deprotonation energy for a series of hydrofullerenes ($C_{60}HBu^t$, $C_{60}H_2$, $C_{60}H_4$,...) for the reaction $C_{60}H_x \rightarrow C_{60}H_{(x-1)}^- + H^+$ has been determined.[18]

In this study, the PA of fullerene (C_{60}) is calculated and the energy of activation for proton transfer is obtained by studying all the possible proton-transfer reactions. The structures and importance of transition states with higher E_a values and their relevance to the proton-transfer reactions of fullerene are explained.

Computational Methods

The calculations were performed using a Gaussian suite of programs developed by Pople and co-workers.[19] In all the calculations, the 6−311+G(2df,p) level theory was used. Earlier calculations using the even more modest B3LYP functional provided reliable results for many systems with the 6−31G(d) basis set,[20] and therefore the proton affinities calculated for C_{60} are also believed to be reliable.

The theoretical framework for calculating the absolute proton affinities (APAs) is given by eqs 1−4. The APA is defined as a negative value of the enthalpy change for the protonation reaction:

$$B + H^+ = B_\alpha H^+ \quad (1)$$

The base and its conjugate acid are denoted by B and $B_\alpha H^+$, respectively, while α denotes the position of proton attack. The absolute proton affinity consists of three terms:

$$APA(B_\alpha) = (\Delta E_{el})_\alpha + (\Delta E_{vib})_\alpha + (5/2)RT \quad (2)$$

$$(\Delta E_{el})_\alpha = E(B) - E(B_\alpha H^+) \quad (3)$$

$$(\Delta E_{vib})_\alpha = E_{vib}(B) - E_{vib}(B_\alpha H^+) \quad (4)$$

Here, $(\Delta E_{el})_\alpha$ is the electronic contribution to proton affinity, E_{vib} includes the zero point vibrational energy (ZPVE) and temperature corrections to the room temperature enthalpy, while $(5/2)RT$ accounts for the translational energy of the proton as well as the $\Delta(pV)$ term. The gas-phase basicity is defined as a Gibbs free energy change of eq 1.[21]

To identify the transition-state geometry, chemical intuition was used to guess the initial position in the calculations for structural optimization. When the stationary point was found, frequency calculations were performed to confirm whether transition states or minima had been determined. Internal reaction coordinate (IRC) calculations were used to confirm the transition states. The E_a barrier was calculated according to eq 5.

$$E_a = (\Delta E_{el})_{TS} + (\Delta ZPE_v)_{TS} \quad (5)$$

where $(\Delta E_{el})_{TS} = [E_{TS}(MH^+) - E_{EQ}(MH^+)]$ and $(\Delta ZPE_v)_{TS} = [ZPE_{TS}(MH^+) - ZPE_{EQ}(MH^+)]$ are the electronic and the ZPE contributions to the PA, respectively. Here, TS denotes transition state and EQ refers to equilibrium structure of protonated fullerene molecule.

Results and Discussion

Geometry optimization was carried out for the fullerene C_{60} within the constraints of I_h symmetry to obtain its global minimum energy structure. The inner proton structures are not reported in this work because of difficulties with the calculation convergence. For protonated C_{60}, geometry optimization was performed within the constraints of C_s to obtain its global minimum energy structure. The protonation site of fullerene is above the carbon atom, which is both expected and in accordance with the protonation site of an isolated benzene ring. The distance between the proton and the nearby carbon atom in the protonated fullerene is 1.11 Å. The calculated PA value, 201.8 kcal/mol, is in good agreement with experimental data,[17] which suggests that the PA value should be between 204 and 207 kcal/mol. The theoretical value lies just below the experimental bracketed values. The counterpoise correction was estimated for the basis set superposition error; for the 6−311+G(2df,p) level basis set this error is an insignificant value of 0.12 kcal/mol.

The structures of all five transition states, TS12_5, TS12_6, TS13_6, TS13_5, and TS14_6, are represented in Figures 1−5. For clarity, only part of C_{60} is shown. Vectors for normal modes, which show the direction of the equilibrium state, are included. In the structural optimizations, the highest possible symmetry of the structures is used. For transition states TS12_6, TS13_5, and TS14_6, symmetry point groups C_{2v}, C_{5v}, and C_{3v} were used, respectively, and are shown in Figures 2, 4, and 5, respectively.

For the two transition states already determined,[14] in one the proton lies above the C−C bond between the five- and six-membered rings (TS12_5; Figure 1), and in the other the proton lies above the C−C bond between two six-membered rings (TS12_6; Figure 2). Three new transition states, TS13_5, TS13_6, and TS14_6, for intramolecular proton transfer were found. In TS13_6 (Figure 3), the proton lies above the six-membered ring between the carbon atoms at positions one and three. In the remaining two transition states, TS13_5 (Figure 4) and TS14_6 (Figure 5), the protons lie above the center of five- and six-membered rings, respectively. The natures of these transition states were verified by frequency calculations, and only one or two negative frequencies were found, whether the saddle was first or second order. The symmetry of the C_{60} molecule means some of the transition states are shared by two equivalent reaction paths, and therefore two negative frequencies are obtained for these transition states. IRC calculations confirmed the reaction path in which a proton transfers from the equilibrium state to the transition state and then back to the equilibrium state. All the calculations were performed in the gas phase, and geometry optimizations were carried out for both equilibrium and transition states.

Tasaki[14] determined TS12_5 and TS12_6 transition states with the B3LYP/6−31+G(2d,p)//HF/6−31G(d) and PM3 levels of theory. The E_a values were 26.75 and 23.06 kcal/mol for a proton-transfer reaction proceeding via TS12_5 and TS12_6 transition states, respectively, at the B3LYP/6−31+G(2d,p)//HF/6−31G(d) level of calculation. In the PM3 level the values were significantly higher, 31.59 and 27.44 kcal/mol for TS12_5

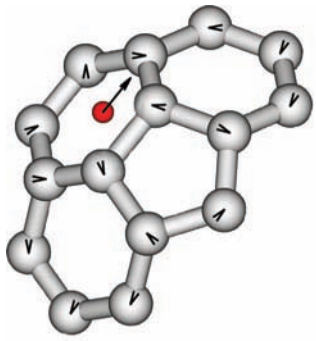

Figure 1. Part of the C_{60} structure for the TS12_5 transition state, with normal modes represented as arrows.

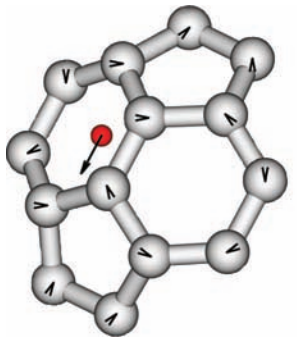

Figure 2. Part of the C_{60} structure for the TS12_6 transition state, with normal modes represented as arrows. C_{2v} symmetry was used for the optimizations.

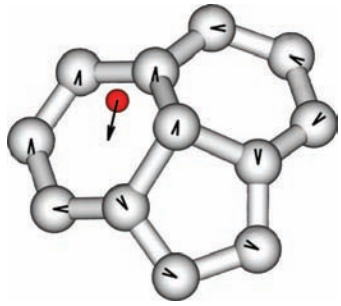

Figure 3. Part of the C_{60} structure for the TS13_6 transition state, with normal modes represented as arrows.

and TS12_6, respectively.[14] Figures 1 and 2 illustrate these two transition states with the vector of the only imaginary frequency showing the direction of proton movement in the proton-transfer reaction. In both cases, the proton is above the C−C bond between either five- and six-membered rings or two six-membered rings. In the structure of the third new transition state found in this study, the proton lies between the center above the six-membered ring and the side between the five- and six-membered rings (TS13_6; Figure 3). In comparison to the transition states TS13_5 and TS14_6, in which the protons are located above the rings and not above the bonds, TS13_6 is the only one that is a first-order saddle point. The vector also shows the movement of the proton from the equilibrium state above the C atom at position 1 to the transition state, and then toward the equilibrium state above the C atom at position 3 (Figure 3). In the TS13_5 and TS14_6 structures, the proton lies above the plane of either the five- or six-membered ring. These two transition states have two imaginary frequencies, which represent transition states on multiple reaction pathways (only the vector toward an equilibrium state is shown). As mentioned above, two transition-state structures were already

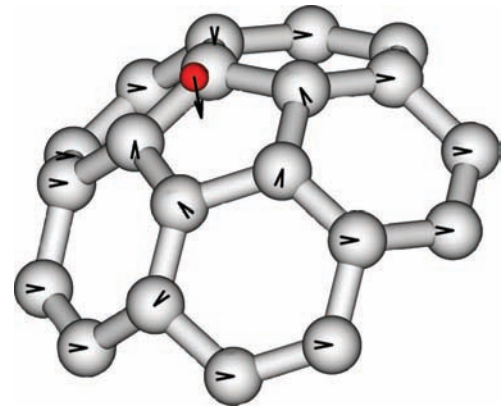

Figure 4. Part of the C_{60} structure for the TS13_3 transition state, with normal modes represented as arrows. C_{5v} symmetry was used for the optimizations.

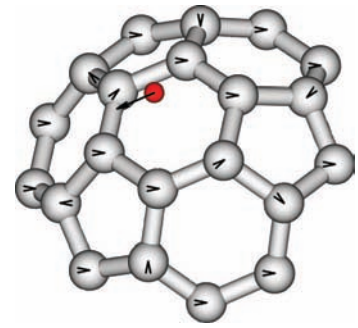

Figure 5. Part of the C_{60} structure for the TS14_6 transition state, with normal modes represented as arrows. C_{3v} symmetry was used for the optimizations.

known, but the other three were determined for the first time in this computation.

The naming of transition states is based on the TS*ab_c* pattern, where *a* and *b* are the start and end positions of proton transfer on the *c*-membered ring. For this nomenclature to be completely correct, TS13_5 and TS14_6 should be first-order transition states. For example, TS14_6 indicates that the transition state for the proton-transfer reaction is from position one to position four in the six-membered ring, but this is not an actual reaction. These transition states are second-order saddle points and represent the middle point at which two reaction paths meet because of the symmetry of the molecule. Thus, the proton transfer from position 1 to position 3 in the five-membered ring or position 1 to position 4 in the six-membered ring is only an apparent reaction, as also seen in the IRC calculations. Table 1 summarizes the results obtained for all the transition states determined.

The distance between the C−C bond and the proton is 1.09 or 1.13 Å in TS12_5 or TS12_6, respectively. Activation energies for these two transition states are 30.2 and 27.9 kcal/mol, respectively. For transition states in which the proton lies above the rings, the distances between the proton and C_{60} are longer than those for transition states in which the proton is located above the bond. The distances range from 1.16 to 1.32 Å above the plane of the rings. These distances are typical for bonds of covalent nature. TS13_6, TS13_5, and TS14_6 have higher E_a values, ranging from 62.6 to 90.0 kcal/mol, than those of TS12_5 and TS12_6. These energies correlate well with the distance from the fullerene molecule; the further the proton is, the larger the E_a.

One can argue that these transition states are not important in terms of their distinctively higher E_a, but they become

TABLE 1: E_a, Distances between the Two Sites that Take Part in the Proton-Transfer Reaction (d), between Proton and C_{60} Molecule (d), and Their Approximate Structure; the Black Dot Represents the Position of the Proton above the Surface of the C_{60} Molecule

transition state	E_a (kcal/mol)	d (Å)	structure
TS12_5	30.16	1.090	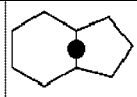
TS12_6	26.86	1.134	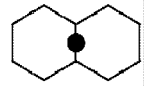
TS13_6	62.57	1.164	
TS13_5	79.92	1.318	
TS14_6	89.99	1.312	

important in the case of functionalized C_{60}. When the functional groups are introduced to enhance the proton conductivity or change C_{60} solubility or to fine-tune any other property of C_{60}, these three transition states might become important. The measurements of the proton conductivity of functionalized C_{60} gave good results, but the mechanisms of proton transfer were not investigated.[13] It remained unknown whether their high proton conductivity is a result of the functional groups attached to fullerene or a property of fullerene itself. Tasaki et al.[8] conducted experiments with hydrogen tricyano fullerene, $HC_{60}(CN)_3$, and characterized its proton conductivity under low humidity conditions.[8,16] This derivative differs from others previously studied in that it has no proton donor or acceptor for proton transfer. Thus, the proton transfer is conducted solely on the fullerene surface. When highly functionalized C_{60} is used, it is not possible for protons to transfer from one carbon atom to the nearest carbon atom, which are the proton-transfer reactions with the lowest E_a. Hence, the importance of the other transition states found in this study. For example, if a proton is in an equilibrium position above one of the C atoms and all the neighboring C atoms are functionalized, then the proton transfer cannot proceed above one of the bonds (the reaction paths with the lowest E_a). The more the C_{60} is functionalized, the more noticeable is the effect.

We also tried to determine the equilibrium structure of protonated C_{60} in which the proton is placed within the C_{60} molecule, but all our attempts were unsuccessful and the calculation did not converge.

Conclusions

Density functional theory was used to calculate the PA of fullerene for the first time. The calculated value, 201.8 kcal/mol, is in good agreement with the available experimental value between 204 and 207 kcal/mol. All the transition states for intramolecular proton transfer in fullerene were determined, three for the first time, and so the complete set of critical points on the $C_{60}H^+$ potential energy surface are known. Activation energy barriers for different proton-transfer reactions are reported and compared; the smallest is around 30 kcal/mol. The transition states with higher E_a values might play a significant role in functionalized C_{60} molecules. Since recently published reports conclude that functionalized fullerenes are promising candidates as functional materials for PEFCs, they warrant further study. For functionalized fullerenes, it has not yet been established whether the proton conductivity depends solely on the functional groups or on fullerene itself, but in such highly functionalized fullerenes the three new transition states reported here could be important.

References and Notes

(1) Saab, A. P.; Stucky, G. D.; Passerini, S.; Smyrl, W. *Fullerene Sci. Technol.* **1998**, *6*, 227.
(2) Hinokuma, K.; Ata, M. *Chem. Phys. Lett.* **2001**, *341*, 442.
(3) Narayanan, S. R.; Yen, S. P.; Liu, L.; Greenbaum, S. G. *J. Phys. Chem. B* **2006**, *110*, 3942.
(4) Hara, M.; Yoshida, T.; Takagaki, A.; Takata, T.; Kondo, J. N.; Hayashi, S.; Domen, K. *Angew. Chem., Int. Ed.* **2004**, *43*, 2955.
(5) Guo, X.; Fang, J.; Watari, T.; Tanaka, K.; Kita, H.; Okamoto, K. *Macromolecules* **2002**, *35*, 6707.
(6) Nicotera, I.; Zhang, T.; Bocarsly, A.; Greenbaum, S. G. *J. Electrochem. Soc.* **2007**, *154*, B466.
(7) Subbaraman, R.; Ghassemi, H.; Zawodzinski, T. A., Jr. *J. Am. Chem. Soc.* **2007**, *129*, 2238.
(8) Tasaki, K.; Venkatesan, A.; Wang, H.; Jousselme, B.; Stucky, G.; Wudl, F. *J. Electrochem. Soc.* **2008**, *155*, 1077.
(9) Tasaki, K. *Progress in Fullerene Research*; Nova Scientific Publishers: New York, 2007.
(10) Tasaki, K.; DeSousa, R.; Wang, H. B.; Gasa, J.; Venkatesan, A.; Pugazhendhi, P.; Loutfy, R. O. *J. Membr. Sci.* **2006**, *281*, 570.
(11) Tasaki, K.; Gasa, J.; Wang, H. B.; DeSousa, R. *Polymer* **2007**, *48*, 4438.
(12) Wang, H. B.; DeSousa, R.; Gasa, J.; Tasaki, K.; Stucky, G.; Jousselme, B.; Wudl, F. *J. Membr. Sci.* **2007**, *289*, 277.
(13) Hinokuma, K.; Ata, M. *J. Electrochem. Soc.* **2003**, *150*, A112.
(14) Tasaki, K. *J. Electrochem. Soc.* **2006**, *153*, A941.
(15) Kreuer, K. D. *Chem. Mater.* **1996**, *8*, 610.
(16) Wang, H.; DeSousa, R.; Gasa, J.; Tasaki, K.; Stucky, G.; Jousselme, B.; Wudl, F. *J. Membr. Sci.* **2007**, *289*, 277.
(17) McElvany, S. W.; Ross, M. M.; Callahan, J. H. *Acc. Chem. Res.* **1992**, *25*, 162.
(18) Choho, K.; Van Lier, G.; Van de Woude, G.; Geerlings, P. *J. Chem. Soc., Perkin Trans. 2* **1996**, 1723.
(19) Frisch, M. J.; Trucks, G. W.; Schlegel, H. B.; Scuseria, G. E.; Robb, M. A.; Cheeseman, J. R.; Montgomery, J. A., Jr.; Vreven, T.; Kudin, K. N.; Burant, J. C.; Millam, J. M.; Iyengar, S. S.; Tomasi, J.; Barone, V.; Mennucci, B.; Cossi, M.; Scalmani, G.; Rega, N.; Petersson, G. A.; Nakatsuji, H.; Hada, M.; Ehara, M.; Toyota, K.; Fukuda, R.; Hasegawa, J.; Ishida, M.; Nakajima, T.; Honda, Y.; Kitao, O.; Nakai, H.; Klene, M.; Li, X.; Knox, J. E.; Hratchian, H. P.; Cross, J. B.; Bakken, V.; Adamo, C.; Jaramillo, J.; Gomperts, R.; Stratmann, R. E.; Yazyev, O.; Austin, A. J.; Cammi, R.; Pomelli, C.; Ochterski, J. W.; Ayala, P. Y.; Morokuma, K.; Voth, G. A.; Salvador, P.; Dannenberg, J. J.; Zakrzewski, V. G.; Dapprich, S.; Daniels, A. D.; Strain, M. C.; Farkas, O.; Malick, D. K.; Rabuck, A. D.; Raghavachari, K.; Foresman, J. B.; Ortiz, J. V.; Cui, Q.; Baboul, A. G.; Clifford, S.; Cioslowski, J.; Stefanov, B. B.; Liu, G.; Liashenko, A.; Piskorz, P.; Komaromi, I.; Martin, R. L.; Fox, D. J.; Keith, T.; Al-Laham, M. A.; Peng, C. Y.; Nanayakkara, A.; Challacombe, M.; Gill, P. M. W.; Johnson, B.; Chen, W.; Wong, M. W.; Gonzalez, C.; Pople, J. A. *Gaussian 03*, revision C.02; Gaussian, Inc.: Wallingford, CT, 2004.
(20) Vessecchi, R.; Galembeck, S. E. *J. Phys. Chem. A* **2008**, *112*, 4060.
(21) Despotović, I.; Kovačević, B.; Maksić, Z. B. *New J. Chem.* **2007**, *31*, 447.

JP8101145